NUMERICAL ANALYSIS OF NATURAL CONVECTION IN A PRISMATIC ENCLOSURE

by

Walid AICH [a*], ***Imen HAJRI*** [b], ***and Ahmed OMRI*** [a]

[a] Unité de Recherche Matériaux, Énergie et Énergies Renouvelables,
Faculté des Sciences de Gafsa, Gafsa, Tunisia
[b] Laboratoire d'Etudes des Systèmes Thermiques et Energétiques,
Ecole Nationale d'Ingénieurs de Monastir, Monastir, Tunisia

Original scientific paper
UDC: 533.6.011:536.25:517.96
DOI: 10.2298/TSCI1102437A

Natural convection heat transfer and fluid flow have been examined numerically using the control-volume finite-element method in an isosceles prismatic cavity, submitted to a uniform heat flux from below. Inclined sides are maintained isothermal and vertical walls are assumed to be perfect thermal insulators, without symmetry assumptions for the flow structure. The aim of the study is to examine a pitchfork bifurcation occurrence. Governing parameters on heat transfer and flow fields are the Rayleigh number and the aspect ratio of the enclosure. It has been found that the heated wall is not isothermal and the flow structure is sensitive to the aspect ratio. It is also found that heat transfer increases with increasing of Rayleigh number and decreases with increasing aspect ratio. The effects of aspect ratio become significant especially for higher values of Rayleigh number. Eventually the obtained results show that a pitchfork bifurcation occurs at a critical Rayleigh number, above which the symmetric solutions becomes unstable and asymmetric solutions are instead obtained.

Keywords: *Rayleigh number, Nusselt number, natural convection, prismatic cavity, heat transfer*

Introduction

It is well known that natural convection heat transfer is occurred due to buoyancy forces and temperature difference in enclosure and this phenomenon can be seen in many energy-related applications, such as thermal insulation of buildings using air gaps, solar energy collectors, furnaces and fire control in buildings and so on. The enclosures encountered in these applications are highly diverse in their geometrical configuration and the most investigated enclosures include the annulus between horizontal cylinders, the spherical annulus, the hollow horizontal cylinder, the closed rectangular cavity, and the closed triangular cavity.

The literature review concerning natural convection in isosceles triangular cavities shows that this configuration was the object of experimental and numerous numerical studies. Earlier, the flow and temperature patterns, local wall heat fluxes, and mean heat flux rates

* Corresponding author; e-mail: aich_walid@yahoo.fr

were measured experimentally by Flack [1, 2] in isosceles triangular cavities with three different aspect ratios. The cavities, filled with air, were heated/cooled from the base and cooled/heated from the inclined walls covering a wide range of Grashof numbers. Asan *et al.* [3] conducted a numerical study of laminar natural convection in a pitched roof of triangular cross-section considering an adiabatic mid-plane wall condition in their numerical procedure. Only summertime conditions were considered over wide ranges of both the Rayleigh number and the height-based aspect ratio. Their results showed that most of the heat exchange takes place near the intersection of the active walls. In another study, they examined the laminar natural convection heat transfer in triangular shaped roofs with different inclination angle and Rayleigh number in winter day. They indicated that both aspect ratio and Rayleigh number affect the temperature and flow field. They also found that heat transfer decreases with the increasing of aspect ratio [4]. The finite-element method was used by Holtzman *et al*. [5] to model the complete isosceles triangular cavity without claiming cavity symmetry. A heated base and symmetrically cooled inclined walls were considered as thermal boundary conditions for various aspect ratios and Grashof numbers. These authors performed a flow visualization study to validate experimentally the existence of symmetry-breaking bifurcations in one cavity of fixed aspect ratio. This anomalous bifurcation phenomenon was intensified by gradually increasing the Grashof number. The main conclusion drawn in this paper was that, for identical isosceles triangular cavities engaging symmetrical and non-symmetrical assumptions, the differences in terms of mean Nusselt number were about 5%. Ridouane *et al*. [6] generated experimental-based correlations for the reliable characterization of the center plane temperature and the mean convective coefficient in isosceles triangular cavities filled with air. The experimental data was gathered from various sources for various aspect ratios and Grashof numbers. Omri *et al*. [7, 8] studied laminar natural convection in a triangular cavity with isothermal upper sidewalls and with a uniform continuous heat flux at the bottom. The study showed that the flow structure and the heat transfer are sensitive to the cavity shape and to the Rayleigh number. An optimum tilt angle was determined corresponding to a minimum of the Nusselt number and for a maximum of the temperature at the bottom center. In recent years, there have been increasing research activities in this area [9-13].

This paper pertains to the natural convection flow in a prismatic cavity with a bottom submitted to a uniform heat flux, two top inclined walls symmetrically cooled and two vertical walls assumed to be adiabatic. The work has been motivated by the heat transfer problem associated with roof-type solar still and various other engineering structures. The present work aims at obtaining the various heat and flow parameters for such enclosures as described above. Results are presented for the steady laminar-flow regime; all the fluid properties are constant except the density variation, which was determined according to the Boussinesq approximation and velocity-pressure formulation without pressure correction was applied. The entire physical domain is taken into consideration for the computations and no symmetry plane is assumed. This step is necessary for the present problem because, as demonstrated experimentally by Holtzman *et al.* [5] for the laminar regime analysis, a pitchfork bifurcation occurs at a critical Grashof number, above which the symmetric solutions becomes unstable and finite perturbations and asymmetric solutions are instead obtained.

Analysis and numerical method

Figure 1 indicates the schematic diagram for the used configuration and geometrical details. The model considered here is a symmetrical room submitted to different boundary conditions. An enclosure is composed by the juxtaposition of an upper prismatic space and a lower rectangular cavity. The horizontal bottom is exposed to a uniform heat flux q while the inclined walls are maintained at a constant temperature T_C and the vertical walls are insulated.

Using the primitive formulation (U, V, P), the governing equations for two-dimensional, laminar incompressible buoyancy-induced flows with Boussinesq approximation and constant fluid properties in non-dimensional velocity-pressure form are:

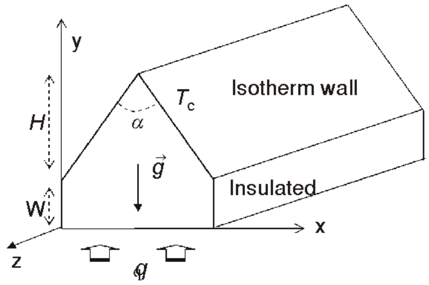

Figure 1. Schematic of an air-filled prismatic cavity

$$\frac{\partial U}{\partial X}+\frac{\partial V}{\partial Y}=0$$

$$U\frac{\partial U}{\partial X}+V\frac{\partial U}{\partial Y}=-\frac{\partial P}{\partial X}+\frac{\partial^2 U}{\partial X^2}+\frac{\partial^2 U}{\partial Y^2}$$

$$U\frac{\partial V}{\partial X}+V\frac{\partial V}{\partial Y}=-\frac{\partial P}{\partial Y}+\frac{\partial^2 V}{\partial X^2}+\frac{\partial^2 V}{\partial Y^2}+\frac{\mathrm{Ra}}{\mathrm{Pr}}\theta$$

$$U\frac{\partial \theta}{\partial X}+V\frac{\partial \theta}{\partial Y}=\frac{1}{\mathrm{Pr}}\left(\frac{\partial^2 \theta}{\partial X^2}+\frac{\partial^2 \theta}{\partial Y^2}\right)$$

where U and V are the velocity components in the X and Y direction, respectively, P – the pressure, and θ – the temperature. In the generated set, the temperature is normalized as:

$$\theta=\frac{k(T-T_C)}{qH}$$

Distances, velocity components, and pressure are normalized by reference, respectively, to:

$$H\frac{\nu}{H} \quad \text{and} \quad \frac{pH^2}{\rho\nu^2}$$

The dimensionless height of the triangular part is then equal to unity (H' = 1) and the dimensionless width of the bottom is:

$$L=\frac{2}{\mathrm{tg}\dfrac{\alpha}{2}}$$

where q is the value of the thermal flux at the bottom, α – the cover tilt angle, and ν – the kinematical viscosity.

A control volume finite elements method [14-17] is used in this computation. The domain of interest is divided in triangular elements and a polygonal volume is constructed around each node by joining the element centre with the middle of sides. The set of governing equations is integrated over the control volume with use of an exponential interpolation in the mean flow direction and a linear interpolation in the transversal direction inside the finite element. The algebraic equations are then solved by the conjugate gradient method. Solutions were assumed to converge when the following convergence criteria was satisfied for every variable at every point in the solution domain:

$$\left|\frac{\varphi_{\text{new}} - \varphi_{old}}{\varphi_{\text{new}}}\right| \leq 10^{-4}$$

where φ represents U, V, P, and θ.

The main purpose of the present study is to report results relevant to steady natural convection in a prismatic cavity. Governing parameters are the Rayleigh number value which changes from 10^3 to 10^6 and the aspect ratio $A_w = W/H$ which changes from 0.25 to 1.

This study is a first part of a research in which we want to understand the 2-D dynamics and we have already proceeded to compute 3-D flows.

The non-dimensional boundary conditions

The solution must satisfy dimensionless boundary conditions which are as:

- at the cover walls: $U = 0$, $V = 0$, and $\theta = 0$,
- at the vertical walls: $U = 0$, $V = 0$ and $\mathrm{d}\theta/\mathrm{d}n = 0$, and
- at the heated horizontal bottom, an external dimensionless thermal flux density $q' = 1$ is considered with $U = 0$, $V = 0$.

We define the local heat transfer coefficient at a given point on the heated wall as:

$$h_{\text{x}} = \frac{q}{T(x) - T_{\text{C}}}$$

where $T(x)$ is the local temperature at this wall. Accordingly the local Nusselt number and the average Nusselt number can be obtained, respectively, as:

$$\text{Nu} = \frac{h_{\text{x}} L}{k} = \frac{1}{\theta(x)}$$

$$\overline{\text{Nu}} = \frac{\overline{h_{\text{x}}} L}{k} = \frac{1}{L}\int_0^L \frac{1}{\theta(x)}\mathrm{d}x$$

where $\theta(x)$ is the local dimensionless temperature.

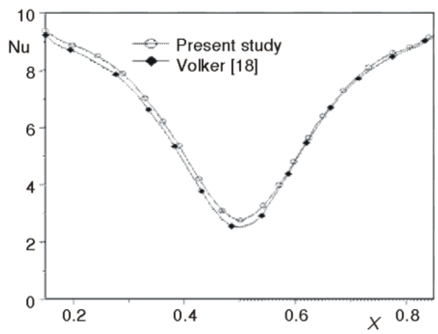

Figure 2. Local Nusselt number on the bottom wall of a triangular cavity

Validation

To validate the numerical analysis, this code is used in the same geometry, with the same boundary conditions used in Volker *et al.* [18]. This geometry is an equilateral triangular cavity heated from below and cooled at the inclined walls. The profile of the local Nu at the bottom in the present study and in Volker *et al.* [18] is compared for Gr = 10^5 and satisfactory agreement was observed as shown in fig. 2. The same code was tested against the experimental results obtained by Holtzman *et al.* [5] by comparing the local Nusselt number for Gr = 10^5 along the bottom of an isosceles triangular enclosure. Excellent agreement was observed as reported in fig. 3.

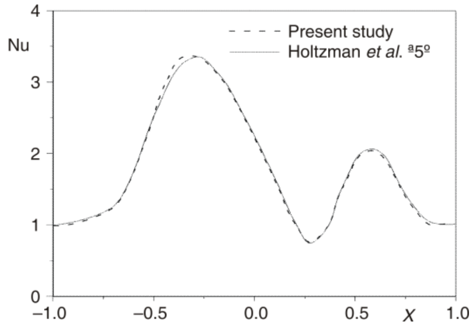

Figure 3. Comparison of results of local Nusselt number on the bottom wall of an isosceles triangular cavity

Results and discussion

In this numerical work, there are some governing parameters, which describe different physical behaviour of the flow and heat transfer by natural convection in a prismatic enclosure such as Rayleigh number value and aspect ratio A_w. In the next subsections, we will discuss the effects of these parameters on the flow and heat transfer characteristics.

Dynamic field

A numerical study was performed to analyze the natural convection heat transfer in a prismatic cavity with different values of Rayleigh number. The following obtained results are investigated for various aspect ratios ranging from 0.25 to 1. Prandtl number is taken as 0.71 which corresponds to air. For lower values of Ra (Ra ≤ 10^4), as shown in fig. 4, two symmetric counter rotating rolls are formed for $A_w \leq 0.75$.

The flow rises along the vertical symmetry axis and gets blocked at the top inclined walls, which turns the flow towards the vertical adiabatic walls. The flow then descends downwards along the sidewalls and turns back horizontally to the central region after hitting the bottom wall. One can see that the two recirculation cells grow in size by increasing the Rayleigh number. The left cell rotates in the anticlockwise sense and the other cell rotates in the clockwise sense. The streamlines become tight at the mid plane indicating that the warmed fluid is accelerated well when buoyancy effects are important. This is demonstrated by fig. 5 giving the vertical velocity component profile and showing that the fluid is pushed upward in the central part of the cavity and is more accelerated at high Ra values.

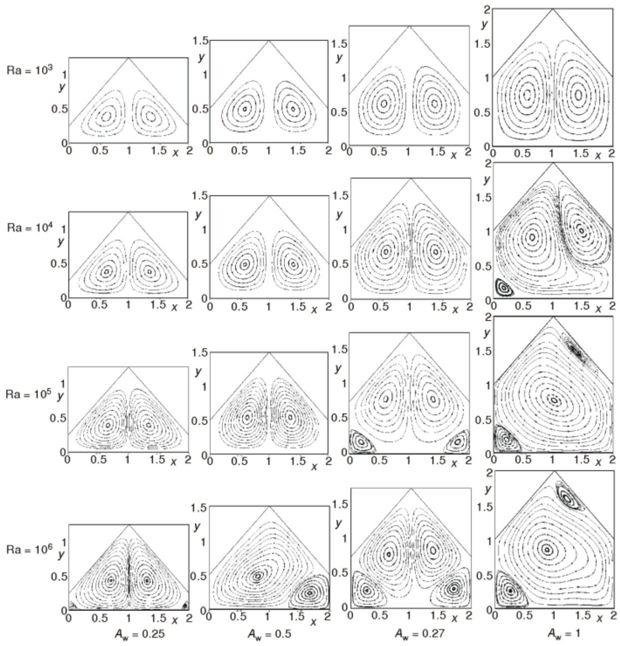

Figure 4. Streamlines for different aspect ratios and different Rayleigh number values

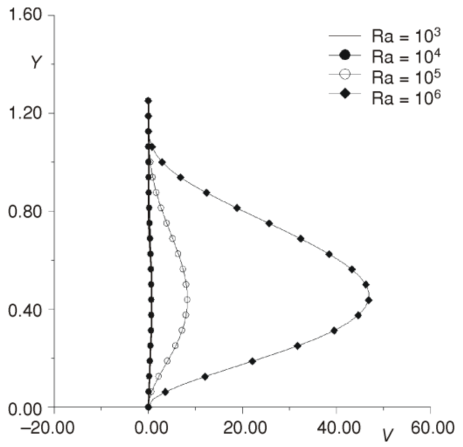

Figure 5. Vertical velocity component profile at the middle for A_w = 0.25 and different values of Rayleigh number

For higher values of Ra (Ra $\geq$ 10^5), the intensity of convection increase and causes secondary vortex to develop on the lower corners of the cavity. Thus we notice the occurrence of pitchfork bifurcation and the flow loses the symmetrical structure and justifies the choice of considering the entire physical domain for the computations.

Figure 6 indicates the profiles of the velocity components along the bottom of the triangular part for different values of Rayleigh number and different aspect ratios. As expected, the values of velocity components are increased by increasing of Rayleigh number. For Ra $\geq$ 10^4, the flow is weak due to quasi-conduction dominant heat transfer regime. Meanwhile, values of velocity decrease with decreasing of the aspect ratios. For Ra $\geq$ 10^5, maximum positive and negative values are almost equal to each other. Sinusoidal velocity profiles are obtained for all parameters.

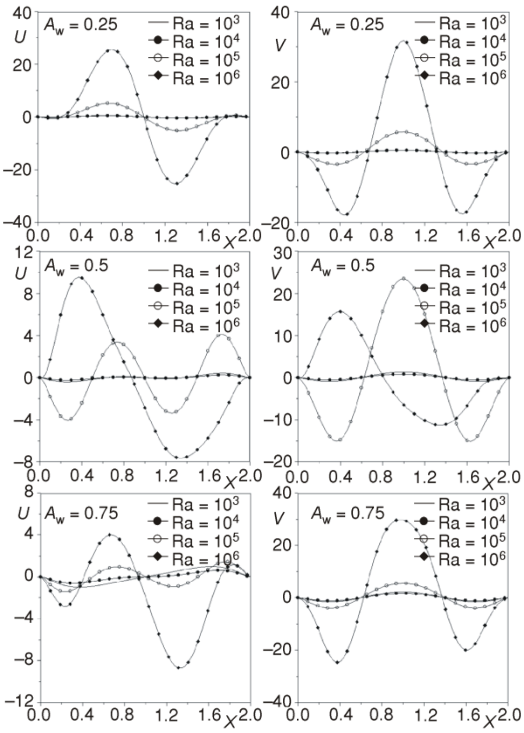

Figure 6. Velocity components profiles along the bottom of the triangular part: horizontal component (left), vertical component (right)

Thermal field

The evolution of the thermal field with Rayleigh number for different aspect ratios is presented in fig. 7. For small Rayleigh numbers (Ra $\geq$ 10^4), the temperature distribution is almost the same as in the pure conduction case. Thus viscous forces are more dominant than the buoyancy forces at lower Ra and diffusion is the principal mode of heat transfer. At higher Ra when the intensity of convection increases significantly, the isotherm patterns changes significantly indicating that the convection is the dominating heat transfer mechanism in the cavity. The effect of aspect ratio on thermal field is more pronounced for higher values of Ra. In fact for Ra $\geq$ 10^6, the increasing of the aspect ratio leads to a plume-like temperature distribution at the right lower corner of the cavity.

Figure 8 shows the temperature profile along the bottom. As it can be seen, the maximum of temperature

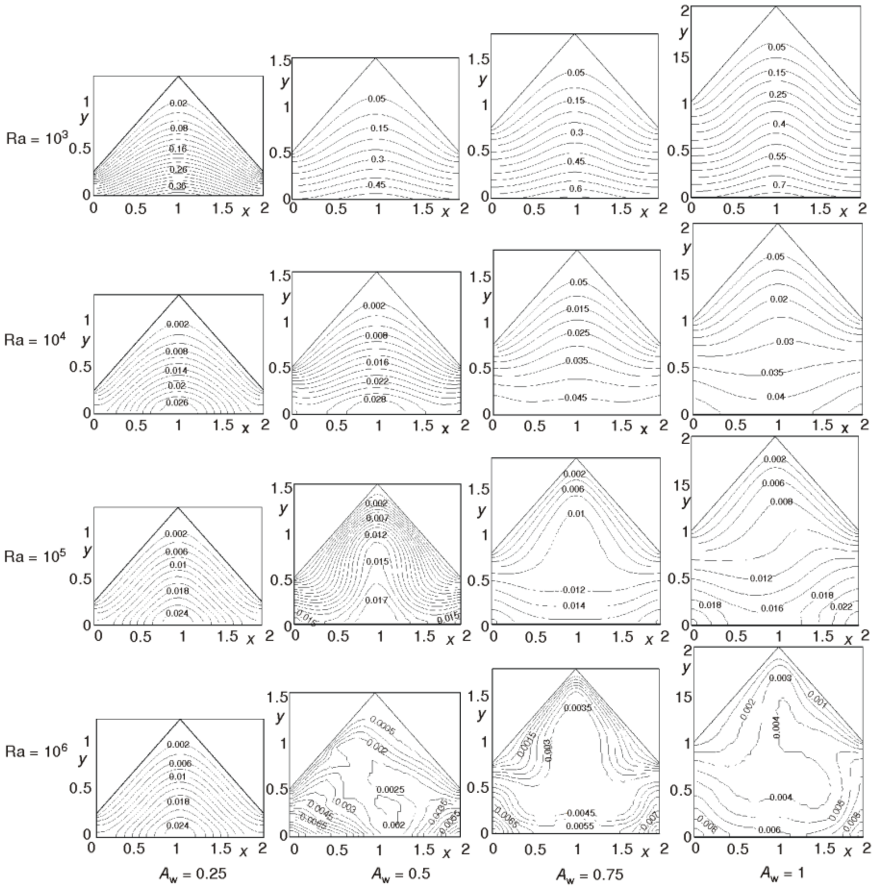

Figure 7. Isotherms patterns for different aspect ratios and different Rayleigh number values

takes place at the middle (stagnation point). For all cases of aspect ratios we have noticed that the temperature decreases by increasing of Rayleigh number as opposed to the variation of the average Nusselt number with Ra. This is due to the fact that the local Nusselt number is reciprocal of the dimensionless surface temperature for the constant heat flux condition. Due to stronger convection, the recirculation zones enlarged by buoyancy forces mixes well the cold fluid and the arisen fluid from the bottom. We have to notice that, in a cavity still receiving a uniform heat flux, the bottom is not isothermal. This is agreed with thermal field structures illustrated previously by fig. 7.

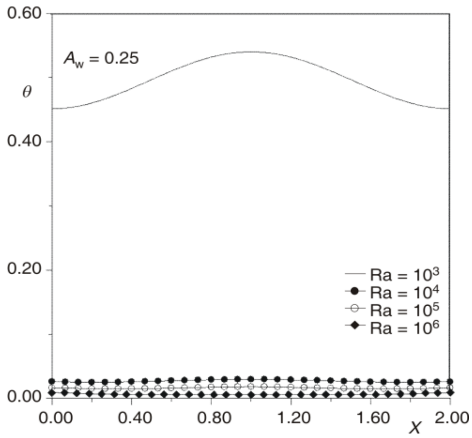

Figure 8. Temperature profile at the bottom A_w = 0.25 and different values of Rayleigh number

The temperature profile at the centerline (symmetry axis) is shown in fig. 9, we have to notice that the flow is characterized by a linear temperature variation in the central region of the cavity. As expected the temperature decreases with the increasing of Ra due to stronger convection and the recirculation zones enlarged by buoyancy forces which mixes well the cold fluid and the arisen fluid from the bottom.

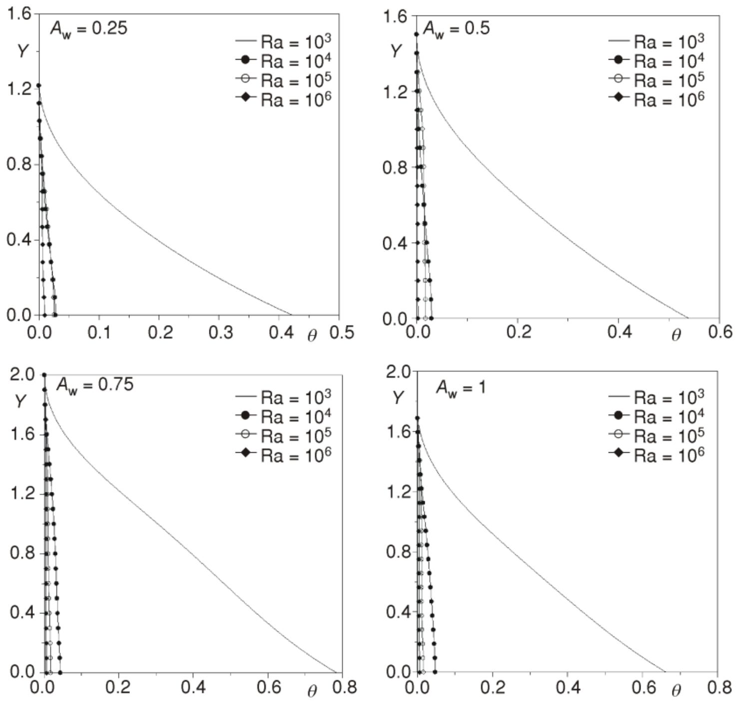

Figure 9. Temperature profile at the centreline for different aspect ratios and different values of Rayleigh number

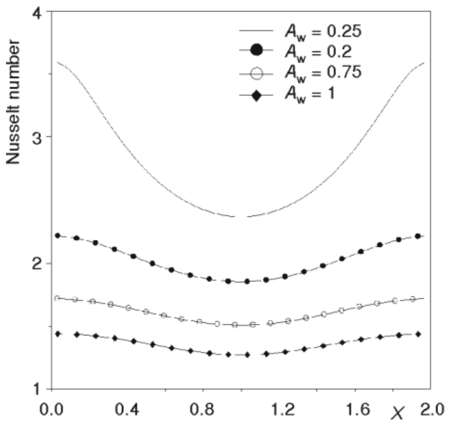

Figure 10. Local Nusselt number at the heated bottom for different aspect ratios

Nusselt number

Effects of aspect ratios on local Nusselt number at the heated bottom are presented in fig. 10 for the same value of Rayleigh number. It is observed that heat transfer was decreased with the increasing of aspect ratio since the volume of enclosure is increased. As expected the Nusselt number admit a minimum at the bottom center where the temperature is maximum. The smallest heat transfer is obtained for the highest aspect ratio due to long distance between hot and cold walls. Thus, the aspect ratio can be a control parameter of the heat transfer.

Variations of the average Nusselt number for heated wall for different aspect ratios and different values of Rayleigh number are presented in fig. 11. As indicated in fig. 10, the value of the average Nusselt is higher for A_w = 0.25 and A_w = 0.5 than that of A_w = 0.75 and A_w = 1 due to small distance between hot and cold walls. It can also be seen that the highest heat transfer is obtained for the highest Rayleigh number. However, the average Nusselt number increases more rapidly for Ra ≥ 10^5 and A_w = 0.25 due to effects of convection heat transfer mode.

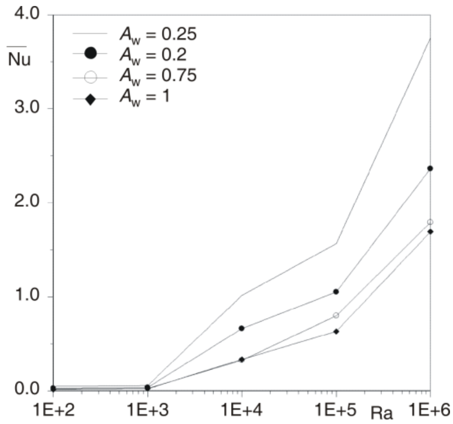

Figure 11. Variation of the average Nusselt number as a function of Rayleigh number for different aspect ratios

Conclusions

The steady-state natural convection heat transfer and flow field inside a prismatic cavity has been numerically examined. Governing parameters, which are effective on temperature and flow field, are the Rayleigh number and the aspect ratio of the enclosure. Based on the obtained results in the present study, the finding can be listed as:

– at the lower Rayleigh number (Ra ≥ 10^4), diffusion is the dominating heat transfer mechanism whereas at higher Rayleigh number (Ra ≥ 10^5 and 10^6) buoyancy driven convection is dominating. As a result, the average Nusselt number at the heated wall does not change significantly for the diffusion dominated case whereas it increases rather rapidly with Ra for the convection dominated case,
– flow and temperature fields are strongly affected by the shape of the enclosure and Rayleigh number play an important role on them,
– heat transfer increases with the increasing of Rayleigh. Multiple circulation cells were obtained at the highest Rayleigh number and the flow loses the symmetrical structure and we notice the occurrence of a pitchfork bifurcation due to stronger convection effects, and
– heat transfer decreases with the increasing of the aspect ratio due to increasing distances between hot and cold walls. Thus, aspect ratio can be a control parameter of heat transfer.

Further study may include the effect of the apex angle of the enclosure, experimental investigations, and three-dimensional turbulent problem.

Acknowledgments

The authors would like to express their deepest gratitude to Mr. Ali Amri and his institution *"The English Polisher"* for their meticulous and painstaking review of the English text of the present paper.

Nomenclature

a	– thermal diffusivity, (= $K/(\rho C_P)$), [m^2s^{-1}]	K	– thermal conductivity, [$Wm^{-1}K^{-1}$]
A_w	– aspect ratio, (= W/H), [–]	Nu	– Nusselt number, [–]
C_P	– specific isobaric heat capacity, [$kg^{-1}K^{-1}$]	$\overline{\text{Nu}}$	– average Nusselt number, [–]
g	– gravitational acceleration, [ms^{-2}]	P	– dimensionless pressure, [–]
H	– height of inclined walls, [m]	Pr	– Prandtl number, [–]
H'	– dimensionless height of inclined walls, [–]	q	– thermal flux density, [Wm^{-2}]

q' – dimensionless thermal flux density, [–]
Ra – Rayleigh number, (= $g\beta qH^4/(K\alpha\nu)$), [–]
U, V – dimensionless velocity components in the X- and Y- directions, [–]
W – height of vertical walls, [m]
X, Y – horizontal and vertical dimensionless co-ordinates, [–]

Greek symbols

α – inclination angle of roofs, $\alpha = 90°$
β – coefficient of volumetric thermal expansion, [K^{-1}]
θ – dimensionless temperature, [–]
ν – kinematic viscosity, [m^2s^{-1}]
ρ – fluid density, [kgm^{-3}]

References

[1] Flack, R. D., Velocity Measurements in Two Natural Convection air Flows Using a Laser Velocimeter, *J. Heat Transfer, 101* (1979), 2, pp. 256-260
[2] Flack, R. D., The Experimental Measurement of Natural Convection Heat Transfer in Triangular Enclosures Heated or Cooled from Below, *J. Heat Transfer, 102* (1980), 4, pp. 770-772
[3] Asan, H., Namli, L., Laminar Natural Convection in a Pitched Roof of Triangular Cross-Section: Summer Day Boundary Condition. *Energy and Buildings, 33* (2000), 1, pp. 69-73
[4] Asan, H., Namli, L., Numerical Simulation of Buoyant Flow in a Roof of Triangular Cross-Section under Winter Day Boundary Conditions, *Energy and Buildings, 33* (2001), 7, pp. 753-757
[5] Holtzman, G. A., Hill, R.W., Ball, K. S., Laminar Natural Convection in Isosceles Triangular Enclosures Heated from Below and Symmetrically Cooled from above, *J. Heat Transfer, 122* (2000), 3, pp. 485-491
[6] Ridouane, E. H., Campo, A., Experimental-Based Correlations for the Characterization of Free Convection of Air Inside Isosceles Triangular Cavities with Variable Apex Angles, *Experimental Heat Transfer, 18* (2005), 2, pp. 81- 86
[7] Omri, A., Orfi, J., Ben Nasrallah, S., Natural Convection Effects in Solar Stills, *Desalination, 183* (2005), 2, pp. 173-178
[8] Omri, A., Orfi, J., Ben Nasrallah, S., Numerical Analysis of Natural Buoyant Induced Regimes in Isosceles Triangular Cavities, *Numerical Heat Transfer, Part A, 52* (2007), 7, pp. 661-678
[9] Hajri, I., Omri, A., Ben Nasrallah, S., A Numerical Model for the Simulation of Double-Diffusive Natural Convection in a Triangular Cavity using Equal Order and Control Volume Based on the Finite Element Method, *Desalination, 206* (2007), 3, pp. 579-588
[10] Varol, Y., Koca, A., Oztop, H. F., Natural Convection Heat Transfer in Gambrel Roofs, *Building and Environment, 42* (2007), 3, pp. 1291-1297
[11] Varol, Y., Oztop, H. F., Yilmaz, T., Natural Convection in Triangular Enclosures with Protruding Isothermal Heater, *International Journal of Heat and Mass Transfer, 50* (2007), 13, pp. 2451–2462
[12] Oztop, H. F., Varol, Y., Koca, A., Laminar Natural Convection Heat Transfer in a Shed Roof with or without Eave for Summer Season, *Applied Thermal Engineering, 27* (2007), 13, pp. 2252-2265
[13] Koca, A., Oztop, H. F., Varol, Y., The Effects of Prandtl Number on Natural Convection in Triangular Enclosures with Localized Heating from Below, *International Communications in Heat and Mass Transfer, 34* (2007), 4, pp. 511-519
[14] Omri, A., Study of Mixed Convection through a Cavity by the Control Volumes Finite Elements Method, Ph. D. thesis, Faculty of Science of Tunis, Tunisia, 2000
[15] Baliga, B. R., A Control-Volume Based Finite Element Method for Convective Heat and Mass Transfer, Ph. D. thesis, University of Minnesota, Minneapolis, Minn., USA, 1978
[16] Baliga, B. R., Patankar, S. V., A Control Volume Finite-Element Method for Two-Dimensional Fluid Flow and Heat Transfer, *Numerical Heat Transfer, 6* (1983), 3, pp. 245-261
[17] Omri, A., Nasrallah, S. B., Control Volume Finite Element Numerical Simulation of Mixed Convection in an Air-Cooled Cavity, *Numerical Heat Transfer, 36* (1999), 6, pp. 615-637
[18] Volker, S., Vurton, T., Vanka, S. P., Finite Volume Multigrid Calculation of Natural Convection Flows on Unstructured Grid, *Numerical Heat Transfer, Part B, 30* (1989), 1, pp. 1-22

Paper submitted: July 20, 2009
Paper revised: December 27, 2009
Paper accepted: January 3, 2010